Electronic Research Archive

http://www.aimspress.com/journal/era

ERA, 33(4): 2148–2171.
DOI: 10.3934/era.2025094
Received: 03 December 2024
Revised: 17 March 2025
Accepted: 27 March 2025
Published: 15 April 2025

Research article

An improved conjugate gradient algorithm by adapting a new line search technique

Asma Maiza[1], **Raouf Ziadi**[1], **Mohammed A. Saleh**[2,*]**and Abdulgader Z. Almaymuni**[2]

[1] Laboratory of Fundamental and Numerical Mathematics (LMFN), Department of Mathematics, University Setif-1-Ferhat Abbas, Setif, Algeria

[2] Department of Cybersecurity, College of Computer, Qassim University, Saudi Arabia

* **Correspondence:** Email: m.saleh@qu.edu.sa.

Abstract: The conjugate gradient (CG) method is an optimization technique known for its rapid convergence; it has blossomed into significant developments and applications. Numerous variations of CG methods have emerged to enhance computational efficiency and address real-world challenges. This work presents a new conjugate gradient method for solving nonlinear unconstrained optimization problems by introducing a new conjugate gradient parameter. To improve the convergence properties, we have proposed a new inexact line search technique that fits in with the suggested approach and can also be useful for other gradient descent methods. The existence of a steplength that meets the new line search conditions is established. The generated descent direction and the convergence properties of the suggested approach are studied under the new line search conditions, where the global convergence is proven under mild assumptions. The proposed approach is evaluated on various test functions, and a comparison with recent similar algorithms is carried out. Furthermore, the proposed algorithm is applied for restoring images with different noise levels.

Keywords: optimization algorithms; conjugate gradient methods; inexact line search technique; global convergence; image processing

1. Introduction

In this study, we consider the following nonlinear optimization problem:

$$f^* = \min_{x \in \mathbb{R}^n} f(x), \tag{P}$$

where $f : \mathbb{R}^n \to \mathbb{R}$ is continuously differentiable. Numerous practical problems in real-life applications can be expressed as unconstrained optimization problems that involve differentiable cost functions [1, 2]. Spotting a solution for these problems becomes difficult when their dimensions are high. CGs are extensively employed to deal with these situations thanks to their low memory requirements and simplicity [3]; they are also widely employed in numerous applications, in particular in image processing [4, 5], designing adaptive filters and learning algorithms [6], neural networks [7], machine learning and signal processing [8, 9], molecular physics [10], and statistical modeling [11]. Starting from a point $x_0 \in \mathbb{R}^n$, the sequence of points $\{x_k\}_{k\in\mathbb{N}} \subset \mathbb{R}^n$ is generated by the following recursive scheme:

$$x_{k+1} = x_k + \alpha_k d_k, \quad k \in \mathbb{N}, \tag{1.1}$$

where d_k is the descent direction and α_k is the steplength that ensures that $f(x_{k+1}) < f(x_k)$. The determination of the steplength α_k is crucial for global convergence. Usually, it is determined using inexact line searches, which guarantee taking steps that should be neither too long nor too short, such as the weak Wolfe line search

$$\begin{aligned} f(x_k + \alpha_k d_k) - f(x_k) &\leq \alpha_k \delta d_k^t g_k, \\ g(x_k + \alpha_k d_k)^t d_k &\geq \sigma d_k^t g_k, \end{aligned}$$

or the strong Wolfe line search

$$\begin{aligned} f(x_k + \alpha_k d_k) - f(x_k) &\leq \alpha_k \delta d_k^t g_k, \\ \left| g(x_k + \alpha_k d_k)^t d_k \right| &\leq -\sigma d_k^t g_k, \end{aligned}$$

where $0 < \delta < \sigma < 1$. The descent search direction d_k is typically computed by the following iterative formula:

$$d_0 = -g_0; \quad d_{k+1} = -g_{k+1} + \beta_k d_k, \quad k \in \mathbb{N}^*,$$

where $\beta_k \in \mathbb{R}$ is the conjugate parameter that characterizes the various conjugate gradient variants. The most famous classical conjugate gradient methods include Hestenes and Stiefel (HS) [12], Fletcher and Reeves (FR) [13], Polak-Ribière-Polyak (PRP) [14, 15], Conjugate Descent (CD) [13], Liu and Storey (LS) [16], and Dai and Yuan (DY) [17], where their parameters β_k are given respectively as follows:

$$\beta_k^{HS} = \frac{g_{k+1}^t y_k}{d_k^t y_k}, \beta_k^{PRP} = \frac{g_{k+1}^t y_k}{\|g_k\|^2}, \beta_k^{LS} = -\frac{g_{k+1}^t y_k}{g_k^t d_k}$$

$$\beta_k^{FR} = \frac{\|g_{k+1}\|^2}{\|g_k\|^2}, \beta_k^{CD} = -\frac{\|g_{k+1}\|^2}{g_k^t d_k}, \beta_k^{DY} = \frac{\|g_{k+1}\|^2}{d_k^t y_k},$$

where $y_k = g_{k+1} - g_k$ and $\|.\|$ denotes the Euclidean norm in $\mathbb{R}^n$. The DY, CD, and FR have better theoretical convergence properties, but practically, they are less effective. Conversely, the LS, HS, and PRP methods are more efficient in practice, but they may not always be convergent.

Due to the difficulty of developing new conjugate gradient formulas with interesting properties, the efforts devoted to combining CG methods to achieve effectiveness and good convergence properties. Numerous works combine conjugate gradient methods; for example, the Touati-Ahmed and Storey (TS) variant [18], the hybrid LS-DY (hLSDY) variant proposed by Liu and Li [19], the hybrid HS-DY (hHSDY) variant proposed by Andrei [20], the hybrid HS-CD (hHSCD) variant proposed by Zheng et al. [21], the hybrid LS-CD (hLSCD) variant proposed by Djordjevic [22], and so on. For more recent hybrid conjugate gradient methods, see [4, 23].

Over the last decade, this research topic has attracted the attention of several researchers and numerous studies have been carried out to develop new efficient conjugate gradient formulas with good numerical performances and global convergent properties. We cite, for example, the RMIL method proposed by Rivaie et al. [24], the WYL method proposed by Wei et al. [25], the NHS and NPRP methods proposed by Zhang [26], the hSM method proposed by Sulaiman-Mohammed [27], and the MHS method proposed by Yao et al. [28], where their parameters β_k are given respectively as follows:

$$\beta_k^{RMIL} = \frac{g_{k+1}^t y_k}{\|d_k\|^2}, \quad \beta_k^{WYL} = \frac{g_{k+1}^t\left(g_{k+1} - \frac{\|g_{k+1}\|}{\|g_k\|} g_k\right)}{\|g_k\|^2},$$

$$\beta_k^{NHS} = \frac{\|g_{k+1}\|^2 - \frac{\|g_{k+1}\|}{\|g_k\|}|g_{k+1}^T g_k|}{d_k^T y_k}, \quad \beta_k^{NPRP} = \frac{\|g_{k+1}\|^2 - \frac{\|g_{k+1}\|}{\|g_k\|}|g_{k+1}^T g_k|}{\|g_k\|^2},$$

$$\beta_k^{hSM} = \frac{g_{k+1}^T(g_{k+1} + g_k)}{\|d_k\|^2}, \quad \beta_k^{MHS} = \frac{g_{k+1}^T\left(g_{k+1} - \frac{\|g_{k+1}\|}{g_k} g_k\right)}{y_k^T g_k}.$$

For more recent conjugate gradient formulas, the reader can see [3, 11].

Inspired by these works, we propose a new conjugate gradient parameter (see Section 2.1 below). Furthermore, to achieve good convergence properties, we have adopted a new inexact line search technique that fits in with the proposed conjugate gradient parameter and can also be useful for other gradient descent methods. The proposed approach converges globally under mild assumptions. The algorithm is successfully applied on a broad set of test functions (with varied analytical expressions and structures) that range from the simplest to the hardest, as well as image processing.

The paper is summarized as follows: the new parameter β_k^{MZ} and the adopted steplength are presented in the next section. The convergence analysis and the global convergence are established in Section 3. The performance of the suggested approach is presented in the last section with some conclusions.

2. The proposed conjugate gradient algorithm

2.1. The new conjugate gradient formula and the corresponding algorithm

Inspired by the RMIL [24] and PRP [15] formulas,

$$\beta_k^{RMIL} = \frac{g_{k+1}^t(g_{k+1} - g_k)}{\|d_k\|^2},$$
$$\beta_k^{PRP} = \frac{g_{k+1}^t y_k}{\|g_k\|^2},$$

we have designed a new parameter, β_k^{MZ} (where "MZ" relates to the authors for easy reference only), which is computed as follows:

$$\beta_k^{MZ} = \frac{g_{k+1}^t \left(g_{k+1} + \frac{||d_k||^2}{||g_k||^2} y_k \right)}{||d_k||^2}. \tag{2.1}$$

Indeed,

$$\begin{aligned} \beta_k^{MZ} &= \frac{g_{k+1}^t g_{k+1} + ||d_k||^2 \frac{g_{k+1}^t y_k}{||g_k||^2}}{||d_k||^2} \\ &= \frac{g_{k+1}^t \left(g_{k+1} + \frac{||d_k||^2}{||g_k||^2} y_k \right)}{||d_k||^2}. \end{aligned}$$

For good convergence properties, we adopt a new inexact line search technique that fits in with the suggested conjugate gradient parameter β_k^{MZ} where the steplength α_k satisfies the following conditions:

$$f(x_k + \alpha_k d_k) - f(x_k) \le \alpha_k \delta d_k^t g_k \frac{||g_k||^2}{||d_k||^2}, \tag{2.2}$$

$$\left| g(x_k + \alpha_k d_k)^t d_k \right| \le -\sigma d_k^t g_k \frac{||g_k||^2}{||d_k||^2}, \tag{2.3}$$

where $\sigma \in \left(0, \frac{\mu-1}{\mu^2(\mu^2+1.2)}\right]$, with $\mu > 1$ and $0 < \delta < \sigma$. Since $\mu > 1$, it results that $0 < \delta < \sigma < 1$. The new line search technique is a modification of the strong Wolfe one by adding the term $\frac{||g_k||^2}{||d_k||^2}$ (to the right side of the strong Wolf inequalities). The new term depends on the gradient values and the descent direction at each point x_k. We have adopted this line search to fit in with the proposed MZ parameter and ensure global convergence with good numerical performance. This modification obtains a steplength that is neither too long nor too short. Also, as shown below, the proposed method exhibits good convergence properties and satisfactory performance. The main steps of the MZ method are sketched in Algorithm 1 below.

Algorithm 1: The MZ algorithm

```
Step 0: (Initialization) Choose a scalar $\mu > 1$ and the parameters $\delta$ and $\sigma$ such that $0 < \delta < \sigma < \frac{\mu-1}{\mu^2(\mu^2+1.2)}$.
        Choose a scalar $\epsilon > 0$ sufficiently small to stop the algorithm. Compute $f(x_0)$, $g_0 = \nabla f(x_0)$ and
        $d_0 = -g_0$. Select a point $x_0 \in \mathbb{R}^n$ and set $k = 0$.
Step 1: If $||g_k|| \le \epsilon$, then stop; otherwise:
        - Compute the steplegth $\alpha_k$ using the new line search technique (2.2) and (2.3).
        - Put $x_{k+1} = x_k + \alpha_k d_k$ and $g_{k+1} = \nabla f(x_{k+1})$.
Step 2: $\beta_k$ computation: Set $y_k = g_{k+1} - g_k$ and compute the conjugate gradient parameter $\beta_k^{MZ}$
        following Eq (2.1).
Step 3: Search direction computation: if the restart criterion of Powell $|g_{k+1}^T g_k| \ge 0.2\,||g_{k+1}||^2$ holds,
        then set $d_{k+1} = -g_{k+1}$; otherwise $d_{k+1} = -g_{k+1} + \beta_k^{MZ} d_k$ and repeat Step 1.
```

2.2. The sufficient descent property

It is well known that the sufficient descent property is crucial for global convergence to hold. To establish it, we first prove the following result that will be required below.

Theorem 2.1. *Let* $\{g_k\}_{k\in\mathbb{N}}$, $\{\beta_k\}_{k\in\mathbb{N}}$ *and* $\{d_k\}_{k\in\mathbb{N}}$ *be the sequences generated by the MZ Algorithm under the conditions* (2.2) *and* (2.3). *Then*

$$\frac{\|g_k\|}{\|d_k\|} \leqslant \mu,\ \forall k \in \mathbb{N}. \tag{2.4}$$

Proof. It is clear that in the case where Powell's restart criterion holds (i.e., $|g_k^t g_{k+1}| \geq 0.2\,\|g_{k+1}\|^2$), the descent direction d_k is defined as $d_k = -g_k$, and the relation (2.4) holds.

Now, if the Powell condition does not hold, we prove the above relation by induction. For $k = 0$, the condition (2.4) holds since $d_0 = -g_0$. Assume the relation (2.4) holds for $k \geq 1$, and let us prove it for $k+1$. Since

$$d_{k+1} = -g_{k+1} + \beta_k^{MZ} d_k, \tag{2.5}$$

by multiplying both sides of (2.5) by g_{k+1}^t, we obtain

$$d_{k+1}^t g_{k+1} = -\|g_{k+1}\|^2 + \beta_k^{MZ} d_k^t g_{k+1}. \tag{2.6}$$

On the other hand, we have

$$\left|\beta_k^{MZ}\right| \leq \frac{\|g_{k+1}\|^2}{\|d_k\|^2} + 1.2\frac{\|g_{k+1}\|^2}{\|g_k\|^2}. \tag{2.7}$$

Indeed,

$$\begin{aligned}
\left|\beta_k^{MZ}\right| &\leq \frac{\|g_{k+1}\|^2}{\|d_k\|^2} + \frac{\left|\|g_{k+1}\|^2 - g_{k+1}^t g_k\right|}{\|g_k\|^2} \\
&\leq \frac{\|g_{k+1}\|^2}{\|d_k\|^2} + \frac{\|g_{k+1}\|^2 + \left|g_{k+1}^t g_k\right|}{\|g_k\|^2} \\
&\leq \frac{\|g_{k+1}\|^2}{\|d_k\|^2} + 1.2\frac{\|g_{k+1}\|^2}{\|g_k\|^2}.
\end{aligned}$$

Hence, from (2.6) and condition (2.3), it follows that

$$\begin{aligned}
\|g_{k+1}\|^2 &\leq \left|d_{k+1}^t g_{k+1}\right| + \left|\beta_k^{MZ}\right| \left|d_k^t g_{k+1}\right| \\
&\leq \left|d_{k+1}^t g_{k+1}\right| + \sigma \left|\beta_k^{MZ}\right| \left|d_k^t g_k\right| \frac{\|g_k\|^2}{\|d_k\|^2} \\
&\leq \|d_{k+1}\|\,\|g_{k+1}\| + \sigma \left|\beta_k^{MZ}\right| \frac{\|g_k\|^3}{\|d_k\|} \\
&\leq \|d_{k+1}\|\,\|g_{k+1}\| + \sigma\left(1.2\frac{\|g_k\|}{\|d_k\|} + \frac{\|g_k\|^3}{\|d_k\|^3}\right)\|g_{k+1}\|^2\,.
\end{aligned} \tag{2.8}$$

Furthermore, since $\sigma \leq \frac{\mu-1}{\mu^2(\mu^2+1.2)}$, we obtain

$$1 - \sigma\left(\frac{\|g_k\|^3}{\|d_k\|^3} + 1.2\frac{\|g_k\|}{\|d_k\|}\right) \geq 1 - \sigma(\mu^3 + 1.2\mu),$$

$$\geq 1 - \frac{\mu - 1}{\mu} = \frac{1}{\mu} > 0, \tag{2.9}$$

by dividing both sides of (2.8) by $\|g_{k+1}\| . \|d_{k+1}\|$, then from (2.9) it results that

$$\frac{\|g_{k+1}\|}{\|d_{k+1}\|} \leq \left(1 - \sigma\left(\frac{\|g_k\|^3}{\|d_k\|^3} + 1.2\frac{\|g_k\|}{\|d_k\|}\right)\right)^{-1} \leq \mu.$$

Thus, the proof is complete. □

Now, we are in the position to prove the sufficient descent condition.

Theorem 2.2. *The sequences* $\{g_k\}_{k\in\mathbb{N}}$, $\{\beta_k\}_{k\in\mathbb{N}}$, *and* $\{d_k\}_{k\in\mathbb{N}}$ *generated by the MZ Algorithm under the new line search conditions* (2.2) *and* (2.3) *with* $\sigma \in \left(0, \frac{\mu-1}{\mu^2(\mu^2+1.2)}\right]$ *and* $\mu > 1$ *satisfy*

$$g_k^t d_k \leqslant -\xi \|g_k\|^2, \quad \forall k \in \mathbb{N}. \tag{2.10}$$

where $\xi > 0$.

Proof. It is evident, in the case where the restart criterion of Powell holds (i.e., $\left|g_k^t g_{k+1}\right| \geq 0.2\|g_{k+1}\|^2$), the descent direction d_k is then given by $d_k = -g_k$, and the relation (2.10) holds.

Now, in the case where the Powell condition does not hold, we prove the above relation by induction. Indeed, for $k = 0$, the search direction $d_0 = -g_0$, which implies that $d_0^t g_0 = -\|g_0\|^2$, and relation (2.10) holds.
Suppose that (2.10) is true for $k \geq 1$. For $k + 1$, by multiplying two sides of (2.5) by g_{k+1}^t, we obtain

$$\begin{aligned}
d_{k+1}^t g_{k+1} &= -\|g_{k+1}\|^2 + \beta_k^{MZ} d_k^t g_{k+1} \\
&\leq -\|g_{k+1}\|^2 + \left|\beta^{MZ}\right| \left|d_k^t g_{k+1}\right| \\
&\leq -\|g_{k+1}\|^2 + \sigma\left(\frac{1.2\,\|g_{k+1}\|^2}{\|g_k\|^2} + \frac{\|g_{k+1}\|^2}{\|d_k\|^2}\right)\|g_k\|\|d_k\|\frac{\|g_k\|^2}{\|d_k\|^2}, \text{(using relations (2.3) and (2.7))} \\
&\leq -\|g_{k+1}\|^2 + \sigma\left(1.2\frac{\|g_k\|}{\|d_k\|} + \frac{\|g_k\|^3}{\|d_k\|^3}\right)\|g_{k+1}\|^2 \\
&\leq -\|g_{k+1}\|^2\left(1 - \sigma(\mu^3 + 1.2\mu)\right) \leq -\frac{1}{\mu}\|g_{k+1}\|^2, \text{(using relations (2.4) and (2.9)).}
\end{aligned}$$

Then the proof is complete for $\xi = \frac{1}{\mu}$. □

3. The convergence analysis

Before analyzing the convergence of the proposed approach, we first show that it is well-defined. In the following theorem, we prove the existence of a steplength α $(0 < \alpha < \infty)$ that meets the conditions (2.2) and (2.3), where $0 < \delta < \sigma$, with $\sigma \in \left(0, \frac{\mu-1}{\mu^2(\mu^2+1.2)}\right]$ and $\mu > 1$.

Theorem 3.1. *Let f be a twice continuously differentiable function that is bounded below. If* $g_k^t d_k < 0$, *then there exists a strictly positive real constant* α *that meets the conditions* (2.2) *and* (2.3).

Proof. Let us define the following function

$$h(\alpha) = f(x_k + \alpha d_k) - f(x_k) - \delta \alpha g_k^t d_k \frac{\|g_k\|^2}{\|d_k\|^2}.$$

Using a standard Taylor development, from relation (2.4), it follows that

$$\begin{aligned} h(\alpha) &= f(x_k + \alpha d_k) - f(x_k) - \delta \alpha g_k^t d_k \frac{\|g_k\|^2}{\|d_k\|^2} \\ &= (f(x_k) + \alpha g_k^t d_k + o(\alpha)) - f(x_k) - \delta \alpha g_k^t d_k \frac{\|g_k\|^2}{\|d_k\|^2}, \\ &= \alpha g_k^t d_k - \delta \alpha g_k^t d_k \frac{\|g_k\|^2}{\|d_k\|^2} + o(\alpha) \\ &\le \alpha \left(1 - \delta \mu^2\right) g_k^t d_k + o(\alpha) \\ &\le \alpha \left(1 - \frac{\mu - 1}{\mu^2 + 1.2}\right) g_k^t d_k + o(\alpha) < 0 \end{aligned}$$

Furthermore, since the function f is lower-bounded, it results that $\lim\limits_{\alpha \to +\infty} h(\alpha) = +\infty$ and $h(0) = 0$. Hence, the function $h(.)$ changes its sign, then there exists a constant $\tau > 0$ such that $h(\tau) = 0$. It is clear that $h(\alpha)$ has a negative sign over the interval $[0, \tau]$, and its global minimum cannot occur at the endpoints since $h(0) = h(\tau) = 0$. Therefore, there exists $\alpha^* \in (0, \tau)$, such that $h(\alpha^*) < 0$ and $h'(\alpha^*) = 0$. Hence

$$h(\alpha^*) = f(x_k + \alpha^* d_k) - f(x_k) - \delta \alpha^* g_k^t d_k \frac{\|g_k\|^2}{\|d_k\|^2} < 0,$$

so that

$$f(x_k + \alpha^* d_k) < f(x) + \delta \alpha^* g_k^t d_k \frac{\|g_k\|^2}{\|d_k\|^2},$$

and the first condition (2.2) holds. On the other hand, we have

$$h'(\alpha) = g_{k+1}^t d_k - \delta g_k^t d_k \frac{\|g_k\|^2}{\|d_k\|^2}.$$

Since $h'(\alpha^*) = 0$, then

$$\sigma g_k^t d_k \frac{\|g_k\|^2}{\|d_k\|^2} \le \delta g_k^t d_k \frac{\|g_k\|^2}{\|d_k\|^2} = g_{k+1}^t d_k < 0,$$

therefore,

$$\left| g_{k+1}^t d_k \right| \le -\sigma g_k^t d_k \frac{\|g_k\|^2}{\|d_k\|^2}.$$

Thus, the second condition (2.3) is also satisfied. □

The global convergence property is crucial for any conjugate gradient method. To establish it, we assume that:

Assumption 3.1. *The level set* $\Omega = \{x \in \mathbb{R}^n | \ f\ (x) \leq f\ (x_0)\}$ *is bounded for any starting point* x_0.

Assumption 3.2. f *is continuously differentiable, whose gradient function* g *satisfies the Lipschitz condition in some closed neighborhood* $\mathcal{N}$ *of* Ω*, i.e.,* $\exists L > 0$ *such that*

$$||g(x) - g(y)|| \leq L\,||x - y|| \qquad \forall x, y \in \mathcal{N}. \tag{3.1}$$

The above assumptions imply the existence of a real number $\Gamma \geq 0$ such that

$$||g_k|| \leq \Gamma \quad \forall x \in \Omega. \tag{3.2}$$

To establish that the MZ algorithm converges globally (see Theorem 3.2 below), we need to prove the following results, which will be needed below.

Lemma 3.1. *Let* $\{g_k\}_{k\in\mathbb{N}}$, $\{\alpha_k\}_{k\in\mathbb{N}}$ *and* $\{d_k\}_{k\in\mathbb{N}}$ *be the sequences generated by the MZ algorithm; then for some* $\varpi > 0$ *we have*

$$g_k^t d_k \geq -\varpi \, ||g_k||^2 \, , \ \forall k \in \mathbb{N}. \tag{3.3}$$

Proof. By multiplying Eq (2.5) by g_{k+1}, we obtain

$$\left| d_{k+1}^t g_{k+1} \right| \leq ||g_{k+1}||^2 + \left| \beta_k^{MZ} \right| \left| d_k^t g_{k+1} \right|.$$

Then, from relation (2.4), it follows that

$$\begin{aligned} \left| d_{k+1}^t g_{k+1} \right| &\leq ||g_{k+1}||^2 + \sigma \left(1.2 \frac{||g_k||}{||d_k||} + \frac{||g_k||^3}{||d_k||^3} \right) ||g_{k+1}||^2 \, , \\ &\leq \left(1 + \sigma \left(1.2\mu + \mu^3 \right) \right) ||g_{k+1}||^2 \, , \end{aligned}$$

which means that,

$$-\varpi \, ||g_{k+1}||^2 \leq d_{k+1}^t g_{k+1} \leq \varpi \, ||g_{k+1}||^2$$

where $\varpi = 1 + \sigma \left(1.2\mu + \mu^3 \right)$ and the proof is complete. □

Lemma 3.2. *Under the above assumptions, the sequence of steplengths* $\{\alpha_k\}_{k\in\mathbb{N}}$ *generated by the MZ algorithm under the new line search conditions* (2.2) *and* (2.3) *with* $\sigma \in \left(0, \frac{\mu-1}{\mu^2(\mu^2+1.2)}\right]$ *and* $\mu > 1$, *satisfies*

$$\alpha_k \geq \frac{\sigma ||g_k||^2 / ||d_k||^2 - 1}{L ||d_k||^2} \, d_k^t g_k, \ \forall k \in \mathbb{N}.$$

Proof. From Theorem 2.1, it follows that

$$\sigma \frac{||g_k||^2}{||d_k||^2} < \frac{\mu - 1}{\mu^2 + 1.2} < 1,$$

hence, from condition (2.3), it results that

$$\left(\sigma \frac{||g_k||^2}{||d_k||^2} - 1 \right) d_k^t g_k < d_k^t (g_{k+1} - g_k) \leq L \alpha_k ||d_k||^2,$$

which completes the proof. □

Lemma 3.3. *Under Assumption 3.1, the sequences $\{g_k\}_{k\in\mathbb{N}}$ and $\{d_k\}_{k\in\mathbb{N}}$ produced by the MZ algorithm satisfy*

$$\sum_{k\geq 0}\frac{(g_k^t d_k)^2}{\|d_k\|^2} < +\infty. \tag{3.4}$$

Proof. Using the condition (2.2) and relation (3.3), we have

$$\begin{aligned} f(x_k) - f(x_k + \alpha_k d_k) &\geq -\delta\alpha_k g_k^t d_k \frac{\|g_k\|^2}{\|d_k\|^2} \\ &\geq \frac{\delta\alpha_k}{\varpi}\frac{(g_k^t d_k)^2}{\|d_k\|^2}. \end{aligned}$$

Then we have,

$$\frac{\delta\alpha_k}{\varpi}\frac{(g_k^t d_k)^2}{\|d_k\|^2} \leq f(x_k) - f(x_{k+1}).$$

Let $m = \min\{\alpha_k : k \in \mathbb{N}\}$; by summing this inequality from $k = 0$ to infinity, we obtain

$$\frac{\delta m}{\varpi}\sum_{k\geq 0}\frac{(g_k^t d_k)^2}{\|d_k\|^2} \leq \sum_{k\geq 0}\frac{\delta\alpha_k}{\varpi}\frac{(g_k^t d_k)^2}{\|d_k\|^2} < +\infty.$$

and the inequality (3.4) holds. □

Theorem 3.2. *Under the above assumptions, the MZ algorithm converges globally in the sense that*

$$\lim_{k\to+\infty}\inf \|g_k\| = 0. \tag{3.5}$$

Proof. Assume that the assertion (3.5) does not hold. Then, there exists a strictly positive value $r > 0$ such that

$$\|g_k\| > r, \ \forall k \in \mathbb{N}. \tag{3.6}$$

Let $m = \min\{\alpha_k : k \in \mathbb{N}\}$ and $D = \max\{\|x - y\| : x, y \in \Omega\}$. From relation (1.1), it results that

$$\|d_k\|^2 = \frac{\|x_{k+1} - x_k\|^2}{\alpha_k^2} \leq \frac{D^2}{m^2}.$$

On the other hand, from (2.7), (3.6), (3.2), and (2.4) we obtain

$$\begin{aligned} d_{k+1} &\leq \|g_{k+1}\| + \left|\beta_k^{MZ}\right| \|d_k\| \\ &\leq \Gamma + \Big(\frac{1.2\Gamma^2}{r^2} + \frac{\mu^2\Gamma^2}{r^2}\Big)\frac{D}{m} = M, \end{aligned}$$

hence,

$$\sum_{k\geq 0}\frac{1}{\|d_k\|^2} = +\infty.$$

But, from (3.6), (2.10), and (3.4), it results that

$$\xi^2 r^4 \sum_{k\geq 0}\frac{1}{\|d_k\|^2} \leq \sum_{k\geq 0}\frac{\xi^2\,\|g_k\|^4}{\|d_k\|^2} \leq \sum_{k\geq 0}\frac{(g_k^t d_k)^2}{\|d_k\|^2} < +\infty,$$

therefore

$$\sum_{k\geq 0}\frac{1}{\|d_k\|^2} < +\infty,$$

which contradicts the claim (3.6), so the assertion (3.5) is true. □

4. Computational experiments

4.1. Application on typical test functions

Here, we present a series of computational performances concerning the MZ algorithm, applied to 84 test functions with 310 test problems, as listed in Table 1 and taken from CUTEr [29] and [30], with dimensions ranging from 2 to 100,000, as well as on restoring four images with different noise levels. All the codes are written and implemented in Matlab. In all experiments, the MZ algorithm is implemented with the setting parameters $\mu = 1.6$, $\delta = 10^{-4}$, and $\sigma = 10^{-3}$.

To demonstrate the effectiveness of the suggested approach, we compared it with HRM [31] with $\theta = 0.4$, NPRP [21], NHS [21], NMFR, MP-CG [32] and CG-DESCENT [33] methods. The methods HRM, NPRP, NHS, and NMFR are implemented using the strong Wolfe conditions, whereas MP-CG and CG-DESCENT are implemented using the weak Wolfe conditions by setting $\delta = 10^{-4}$ and $\sigma = 10^{-3}$ (the other parameters are set as default as taken in [32]). For this comparison, the same starting point is assigned for each test problem, and each implementation is considered successful if a point x_k where $\|g(x_k)\|_\infty \leq 10^{-6}$ is reached within 2000 iterations, with CPU time less than 500 seconds; alternatively, the implementation is assigned as a failure.

Throughout the numerical results, in Figures 1–4, we compare the performance of the proposed method with NPRP, HRM, NHS, NMFR, MP-CG, and CG-DESCENT methods using the logarithmic performance profile of Dolan and Moré [34], relative to the number of iterations, function evaluations, gradient evaluations, and CPU-time. For a solver s, we define the ratio

$$r_{\text{P},s} = \frac{N_{\text{P},s}}{\min\{N_{\text{P},s} : s \in S\}},$$

where $N_{\text{P},s}$ denotes either the number of iterations, the number of function (gradient) evaluations, or the CPU time required by the solver s to solve a problem P. If a solver s does not solve the problem P, the ratio $r_{\text{P},s}$ is assigned a large number. The logarithmic performance profile for each solver s is defined as follows:

$$\rho_s(\tau) = \frac{\text{number of problems where } \log_2(r_{\text{P},s}) \leq \tau}{\text{total number of problems}},$$

For each method, we plot the fraction $\rho_s(\tau)$ of problems for which the method has a number of iterations (resp. number of function (gradient) evaluations and CPU time) that is within a factor τ. The curve that is shaped on the top corresponds to the code that solves the majority of the test problems within the given factor τ; for more details, see [34].

Figures 1–4 illustrate that the MZ method outperforms the others; notably, it is faster for approximately 36% of the test problems and successfully solves around 97% of them, followed by the CG-DESCENT method with 96% of test problems. The NPRP, MP$^+$-CG, and NMFR methods have solved 93% of test problems with superiority to the MP$^+$-CG method, whereas HRM and NHS solved respectively, about 91% and 86% of the test problems. These outcomes prove the competitiveness and rapid convergence of the MZ algorithm in the majority of the test problems.

Table 1. List of test functions.

Function	Dimension *n*	Function	Dimension *n*
Extended Maratos	500, 700, 1000,2000,4000, 9000, 9500, 60,000, 10,000, 15,000	Arwhead	50, 60, 80, 100, 150, 200, 800, 1000, 5000
COSINE	10, 100 , 500, 1000	SINE	10, 100 , 500, 1000
ENGVAL1	100, 600, 800, 1000, 1500, 1600,1800, 10,000	Diagonal 1	2,10, 100, 1000, 10,000, 100,000
Generalized Tridiagonal 1	2, 10, 20,300, 500, 700, 10,000	FLETCHCR	2, 4
Extended White and Holst	1000, 2000, 3000, 4000, 5000, 6000	Diagonal 2	2, 4, 10, 800, 1000, 80,000
Diagonal 7	500, 700, 1000, 1500, 2000, 7000, 8000	Extended Rosenbrock	10, 20,100 ,1200, 3000, 4000, 5000
Quadratic QF2	100, 200,1000,5000, 7000, 9000, 10,000, 50,000	Diagonal 8	100, 200, 400, 500, 1000, 1500, 2000
Extended Freudenstein and Roth	10, 100, 1000, 4000, 9000, 10,000, 20,000, 50,000, 60,000, 80,000	Diagonal 3	2, 4, 6, 10, 50, 100, 200, 400, 700
DENSCHNF	10, 100, 10,000, 25,000, 30,000 50,000, 70,000, 80,000, 90,000	Extended Himmelblau	4, 6,10, 9000, 10,000
Perturbed Quadratic	2	POWER	2
QUARTC	2	Raydan 1	2
Generalized Rosenbrock	2, 50, 800, 1000	Perturbed quadratic diagonal	2
DENSCHNB	10, 90, 100, 2000, 3000, 4000, 5000, 6000, 7000, 9000	Raydan 2	1000, 4000, 50,000,80,000
HIMMELBG	2000, 3000, 6000, 30,000, 50,000, 80,000	LIARWHD	10,50, 4000,5000, 5500, 10,000, 20,000, 80,000
Extended quadratic exponential EP1	40,000, 50,000, 60,000, 70,000	Diagonal 5	100, 200, 700, 1000, 1500, 2000, 2200, 2500
Extended BD1	4, 800, 900, 2000, 3000, 5000 20,000, 40,000, 60,000, 70,000, 80,000	Extended quadratic penalty QP1	4, 6, 8, 10, 50, 100, 700, 1000, 1500
Hager	2, 4,10,50, 80, 150, 300	NONSCOMP	2, 4, 1000, 5000, 70,000
HIMMELLH	10, 50, 300, 500, 10,000, 50,000, 60,000, 80,000, 10,000	Quadratic QF1	5000, 6000, 8000, 9000, 20,000, 50,000, 70,000, 80,000
Extended quadratic penalty QP2	40, 60, 200	Diagonal 4	20,000, 30,000, 40,000, 50,000, 60,000, 70,000
DIXON3DQ	2, 4, 600	Extended PSC1	2, 4, 10, 100, 1000,10,000
Almost Perturbed Quadratic	2, 4, 6	Diagonal 9	10, 30,50, 60, 70, 90
Extended Tridiagonal 1	6, 10, 20,80, 90, 100, 150, 300, 500, 700, 1000, 5000, 6000	NONDIA	10, 100,500,1000,5000,100,000
EIGENALS	2550	BDQRTIC	5000
EIGENBLS	2550	EIGENCLS	2652
BROYDN7D	5000	BRYBND	5000
CHENHARK	5000	CHAINWOO	4000
EXTROSNB	1000	ENGVAL1	5000
ENGVAL2	3	ERRINROS	50
EXTROSNB	1000	FLETCBV2	5000
FLETCBV3	5000	FLETCHBV	5000
ROSENBR	2	S308	2
SPMSRTLS	4999	DIXMAANE	3000
DIXMAANF	3000	DIXMAANG	3000
DIXMAANH	3000	JENSMP	2
VAREIGVL	50	DIXMAANI	3000
KOWOSB	4	VIBRBEAM	8
DIXMAANJ	3000	LIARWHD	5000
WATSON	12	DIXMAANK	3000
LOGHAIRY	2	WOODS	4000
HILBERTA	2	TOINTGOR	50
HIMMELBB	2	TOINTPSP	50
HIMMELBF	4	TOINTQOR	50

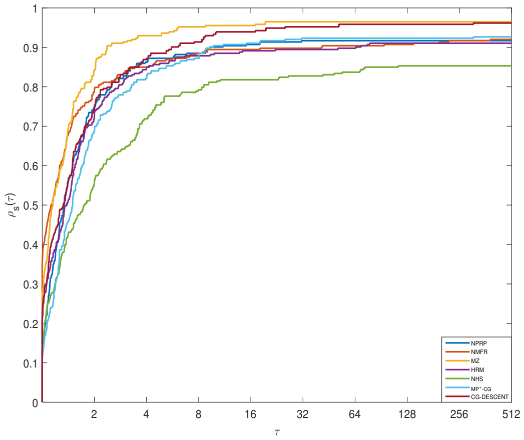

Figure 1. Performance profiles plot based on CPU time.

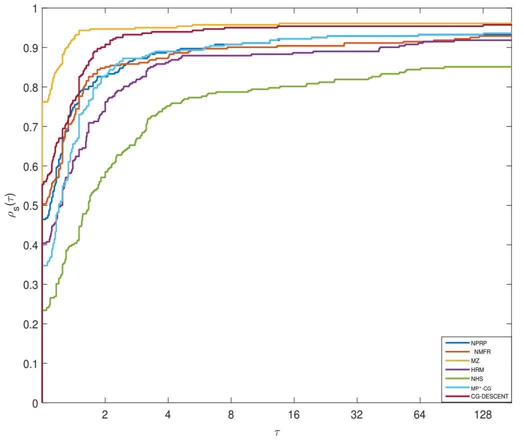

Figure 2. Performance profiles plot based on the number of iterations.

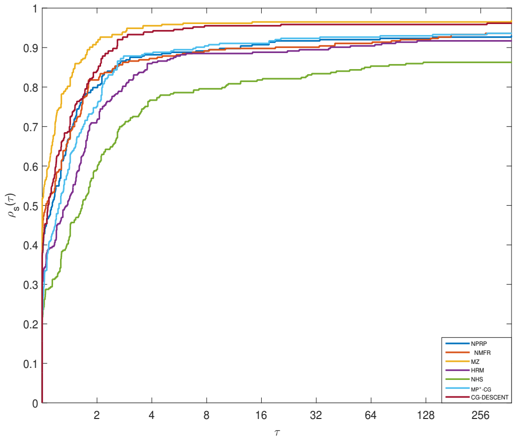

Figure 3. Performance profiles plot based on the number of function evaluations.

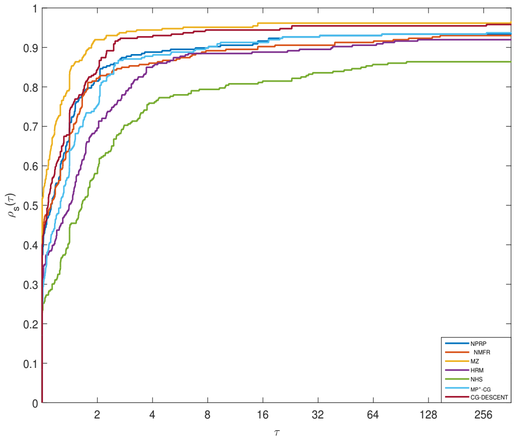

Figure 4. Performance profiles plot based on the number of gradient evaluations.

4.2. Image restoration problems

In optimization fields, image restoration problems are considered among the most difficult ones; they aim to restore the original image from one that has been corrupted by impulse noise. For this comparison, four test images (Man.png, Boat.png, Lena.jpg, and Bridge.bmp) of size 512 × 512 are chosen to evaluate the effectiveness of the MZ algorithm against the same variants used in the previous comparisons. The image quality is assessed by two factors: the peak signal-to-noise ratio (PSNR) and its relative error (Err),

$$PSNR = 10\log_{10}\frac{M \times N \times 255^2}{\sum_{i,j}(x^r_{i,j} - x^*_{i,j})^2}, \qquad Err = \frac{\|x^r - x^*\|}{\|x^*\|}$$

where M and N are the sizes of the image, $x^r_{i,j}$ represents the pixel values of the restored image, and $x^*_{i,j}$ denotes the original pixel values. The setting parameters of the proponent algorithms are set similarly to the previous test, and each computation will stop if any of the following criteria are fulfilled:

$$Iter > 300 \text{ or } \frac{|f(x_{k+1} - f(x_k)|}{|f(x_k)|} < 10^{-4}.$$

Figures 5–10 show the restored images by impulse 30 %, 50%, and 70 % of noise. The performance of each algorithm is measured by the restored image quality, the elapsed time, and the number of iterations. The numerical outcomes are reported in Tables 2–4. The algorithm with a high PSNR and minimal error with less CPU time is considered the best.

Upon examining the results in Tables 2–4 and Figures 5–10, it becomes evident that the MZ algorithm delivers good performance. In fact, as illustrated in Table 2 and Figures 5 and 6, we can observe that the NHS, NPRP and MP-CG methods failed to restore images with 30% noise, whereas the other methods were successful with a PSNR greater than 25, and the MZ method has the highest PSNR value for the Man and Bridge images. On the other hand, the visual outcomes of Figures 7 and 8 with 50% noise show that the NHS, NPRP, and MP-CG methods also failed to remove the noise with a PSNR less than 25, while the HRM, MZ, NMFR, and CG-DESCENT methods succeeded in restoring all the images and the bold values in Table 3 indicate the superiority of the MZ method for restoring three images. For 70% noise, as shown in Figures 9 and 10, and Table 4, the NHS, NPRP, and MP-CG methods failed to restore the original images; the HRM method succeeded in removing the noise from the Boat and Bridge images, and the NMFR method succeeded in restoring the images of Man, Boat, and Lena, while the MZ and CG-DESCENT methods succeeded in removing the noise from all images, where the highest PSNR value corresponds to the MZ method.

On the whole, the numerical and visual outcomes of removing 30%, 50%, and 70% of noise show a satisfactory performance of the MZ algorithm. Notably, the bold values in Tables 2–4 highlight the efficiency of the proposed algorithm and take a short time to restore the majority of the test images.

Table 2. Numerical results for image restoration problems with 30% salt-and-pepper.

Images Methods		Man	Boat	Lena	Bridge
NHS	Iter	26	26	25	23
	CPU	15.7869	14.9272	14.5193	14.4291
	PSNR	15.7231	17.5183	17.3303	16.2491
	Err	0.3405	0.2462	0.2993	0.3110
NMFR	Iter	18	16	15	35
	CPU	13.5430	12.8837	13.1202	16.5120
	PSNR	31.5222	33.6216	37.6712	28.4505
	Err	0.0552	0.0385	0.0287	0.0763
HRM	Iter	13	14	16	19
	CPU	14.4333	16.1088	15.9510	18.3902
	PSNR	31.4316	33.5530	**37.7937**	28.5705
	Err	0.0558	0.0388	**0.0283**	0.0752
NPRP	Iter	6	6	6	6
	CPU	12.4714	12.5510	**11.1241**	12.1049
	PSNR	15.7089	17.5182	17.3155	16.2439
	Err	0.3410	0.2461	0.2998	0.3111
MZ	Iter	15	27	18	20
	CPU	16.3077	13.2510	12.3024	17.5385
	PSNR	**31.5635**	33.1524	37.6352	**28.5895**
	Err	**0.0458**	0.0423	0.0296	**0.07401**
MP-CG	Iter	**4**	**4**	**4**	**4**
	CPU	**12.0037**	**11.4063**	11.5515	**11.8034**
	PSNR	15.7392	17.5272	17.3172	16.2386
	Err	0.3398	0.2459	0.2997	0.3113
CG-DESCENT	Iter	17	17	17	16
	CPU	14.0641	13.9686	14.3062	16.8352
	PSNR	31.5597	**33.6639**	**37.7533**	28.5640
	Err	0.0549	**0.0383**	**0.0285**	0.0753

5. Conclusions

In this paper, we propose a new conjugate gradient algorithm by introducing a novel conjugate gradient parameter for solving nonlinear unconstrained optimization problems. To speed up the convergence, we have adopted a new inexact line search technique that fits in with the proposed conjugate gradient parameter. The existence of a steplength that meets the new line search conditions is established, and the generated search direction d_k satisfies the sufficient descent condition. The convergence properties of the suggested approach are analyzed under the new line search conditions, and the proposed method converges globally under mild assumptions. Numerical experiments are carried out on 310 test functions and four image restoration problems with three noise levels. The numerical comparison with similar and recent CG methods shows that the proposed algorithm is competitive and efficient for solving large-scale complex problems as well as image restoration ones.

Table 3. Numerical results for image restoration problems with 50% salt-and-pepper.

Images Methods		Man	Boat	Lena	Bridge
NHS	Iter	31	34	33	30
	CPU	24.3502	24.8263	24.8593	23.0874
	PSNR	13.4363	15.2070	14.7535	14.1568
	Err	0.4430	0.3212	0.4027	0.3957
NMFR	Iter	22	17	17	18
	CPU	20.1598	**18.0440**	18.1020	17.7847
	PSNR	29.1302	31.0974	35.0066	26.5072
	Err	0.072728	0.051554	0.039116	0.095465
HRM	Iter	19	14	26	14
	CPU	31.6329	22.9351	33.0992	21.4267
	PSNR	29.0482	30.0439	35.0633	26.2812
	Err	0.073418	0.058202	**0.038862**	0.097982
NPRP	Iter	**6**	**6**	**6**	**5**
	CPU	**16.0684**	18.4926	**16.6391**	**16.2163**
	PSNR	13.4675	15.1712	14.7757	14.1672
	Err	0.441405	0.322532	0.401702	0.395223
MZ	Iter	19	22	22	21
	CPU	27.0201	22.20145	24.2571	24.3507
	PSNR	**29.1725**	**31.1735**	**35.1438**	26.6304
	Err	**0.0723**	**0.0523**	**0.0393**	0.0943
MP-CG	Iter	**6**	**6**	**6**	**5**
	CPU	18.9429	19.0158	18.4746	16.5455
	PSNR	13.4606	15.2050	14.7792	14.1677
	Err	0.4417	0.3212	0.4015	0.3952
CG-DESCENT	Iter	22	19	20	23
	CPU	26.4330	23.1224	21.7718	29.0420
	PSNR	29.1528	31.1018	35.0045	**26.7484**
	Err	0.0725	0.0525	0.0395	**0.0935**

Table 4. Numerical results for image restoration problems with 70% salt-and-pepper.

Images Methods		Man	Boat	Lena	Bridge
NHS	Iter	34	37	34	31
	CPU	29.7937	30.6846	27.8669	22.3260
	PSNR	11.3935	12.9901	12.5870	12.1899
	Err	0.5604	0.4146	0.5168	0.4963
NMFR	Iter	24	23	20	25
	CPU	24.9760	23.0873	**13.6592**	25.6359
	PSNR	26.2295	28.1877	28.5882	24.4006
	Err	0.101563	0.072068	0.075126	0.121667
HRM	Iter	10	26	20	25
	CPU	28.8301	49.0126	40.3861	48.7749
	PSNR	22.3136	28.1401	30.0993	24.2470
	Err	0.159416	0.072465	0.068821	0.123838
NPRP	Iter	**6**	**6**	**6**	**6**
	CPU	**22.5660**	**20.0892**	20.4119	**19.4860**
	PSNR	11.3863	13.0485	12.5869	12.1776
	Err	0.560914	0.411816	0.516821	0.496963
MZ	Iter	33	30	29	37
	CPU	27.2350	27.0357	26.4757	30.5668
	PNSR	**26.5342**	**28.2927**	**32.9605**	**25.5351**
	Err	**0.1003**	**0.071202**	**0.0424**	**0.1020**
MP-CG	Iter	**6**	**6**	**6**	7
	CPU	22.9555	24.2128	23.7843	26.3187
	PNSR	11.4052	13.0353	12.6075	12.1781
	Err	0.5596	0.4124	0.5156	0.4969
CG-DESCENT	Iter	23	23	26	18
	CPU	32.5424	34.5871	34.7645	29.9523
	PNSR	26.2393	28.2483	31.7190	24.3003
	Err	0.1014	0.0715	0.0571	0.1230

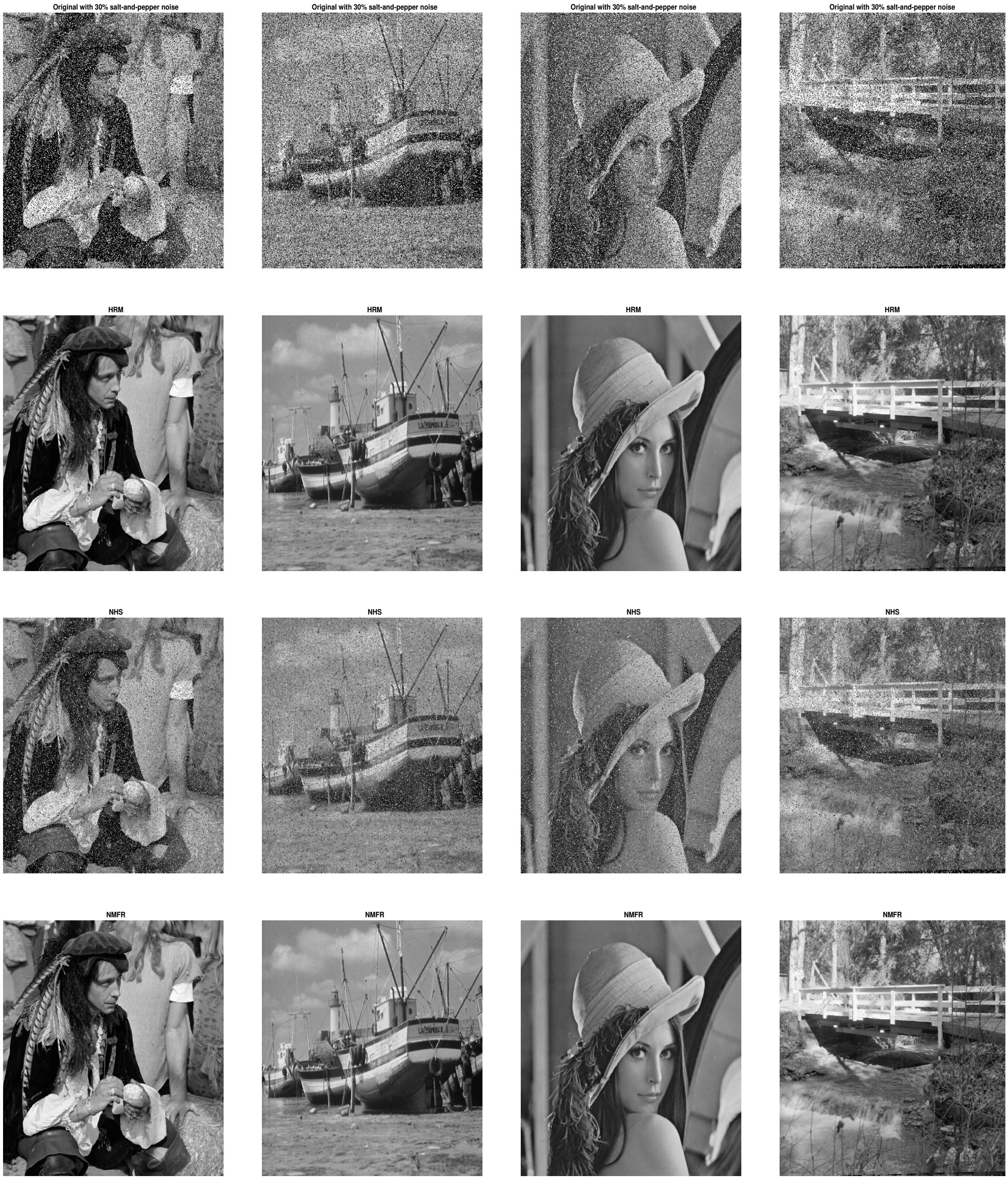
Original with 30% salt-and-pepper noise
Original with 30% salt-and-pepper noise
Original with 30% salt-and-pepper noise
Original with 30% salt-and-pepper noise
HRM
HRM
HRM
HRM
NHS
NHS
NHS
NHS
NMFR
NMFR
NMFR
NMFR

Figure 5. The noisy images with 30% salt-and-pepper (first row) and the restored images by HRM (second row), NHS (third row), and NMFR (last row).

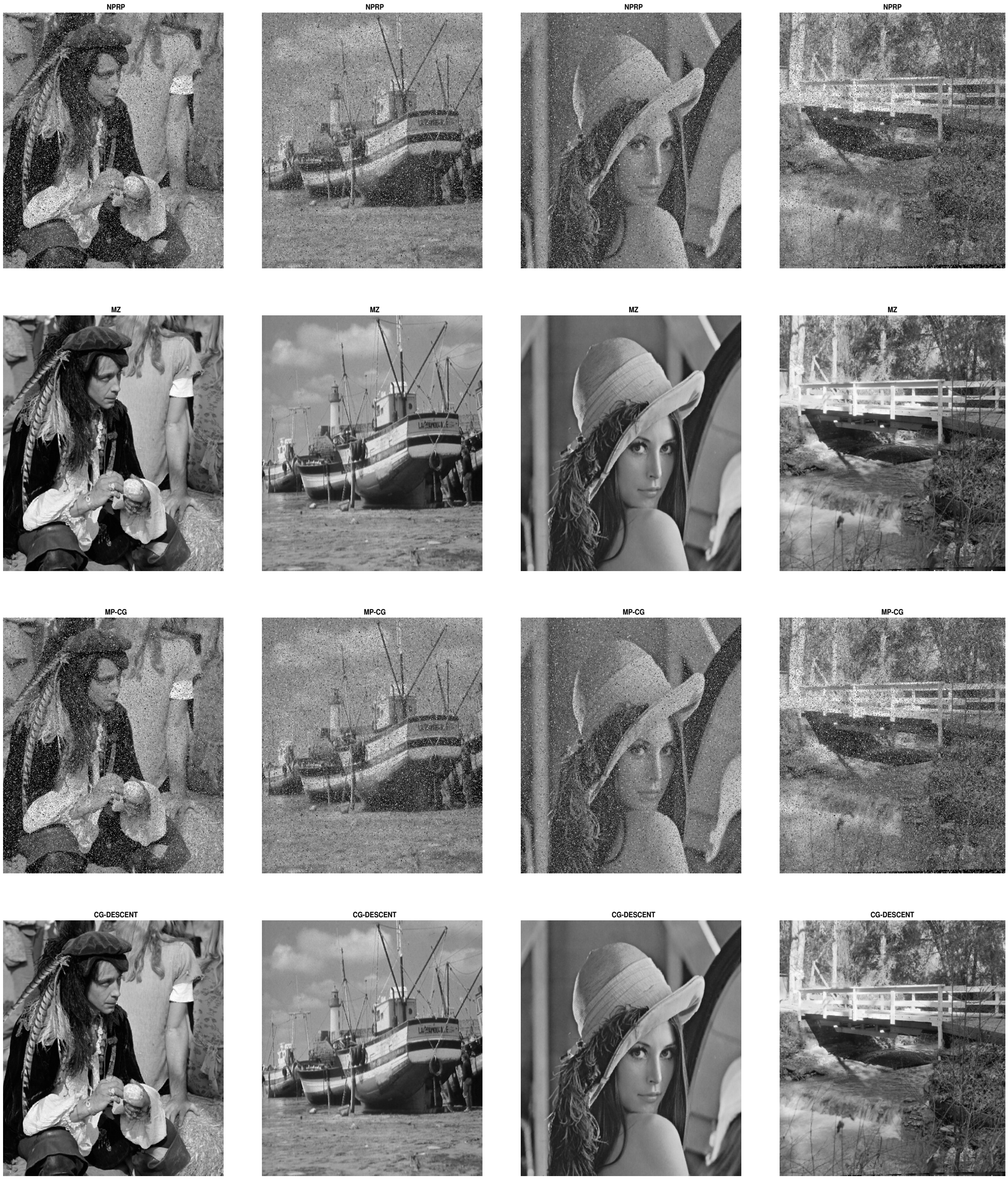

Figure 6. The restored images with 30% salt-and-pepper by NPRP (first row), MZ (second row), MP-CG (third row), and CG-DESCENT (last row).

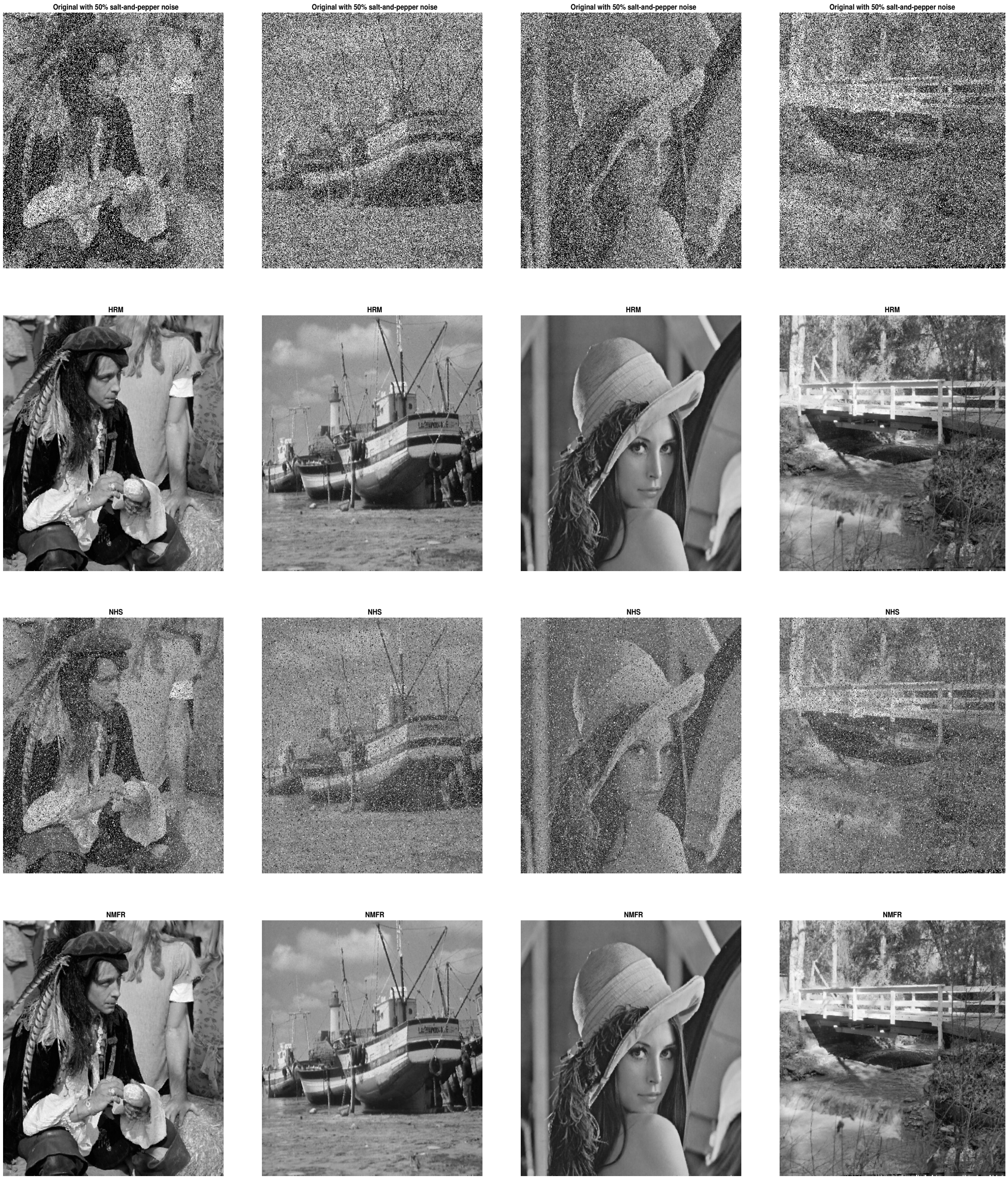
Original with 50% salt-and-pepper noise
Original with 50% salt-and-pepper noise
Original with 50% salt-and-pepper noise
Original with 50% salt-and-pepper noise
HRM
HRM
HRM
HRM
NHS
NHS
NHS
NHS
NMFR
NMFR
NMFR
NMFR

Figure 7. The noisy images with 50% salt-and-pepper (first row) and the restored images by HRM (second row), NHS (third row), and NMFR (last row).

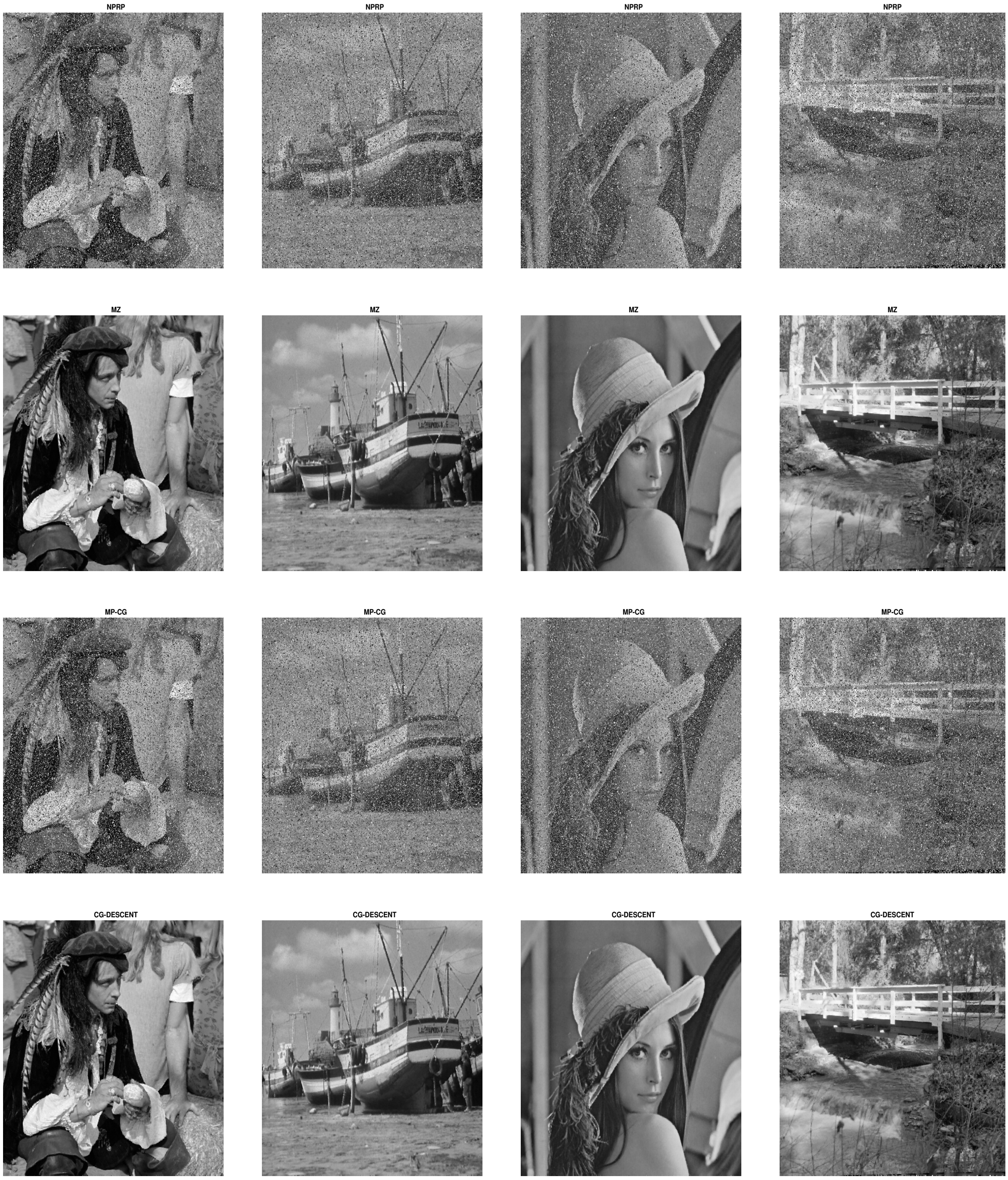

Figure 8. The restored images with 50% salt-and-pepper by NPRP (first row), MZ (second row), MP-CG (third row), and CG-DECENT (last row).

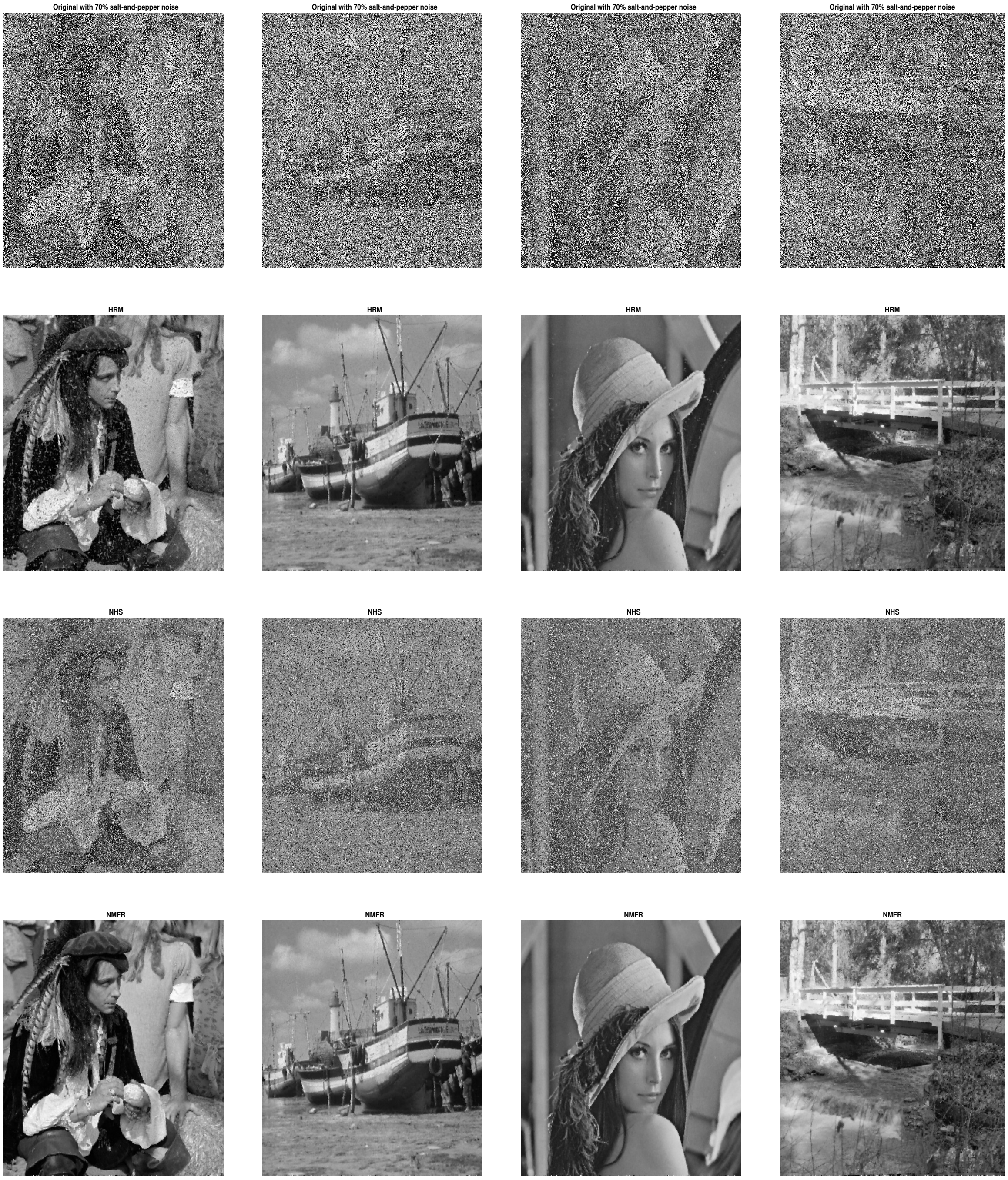
Original with 70% salt-and-pepper noise
Original with 70% salt-and-pepper noise
Original with 70% salt-and-pepper noise
Original with 70% salt-and-pepper noise
HRM
HRM
HRM
HRM
NHS
NHS
NHS
NHS
NMFR
NMFR
NMFR
NMFR

Figure 9. The noisy images with 70% salt-and-pepper (first row) and the restored images by HRM (second row), NHS (third row), and NMFR (last row).

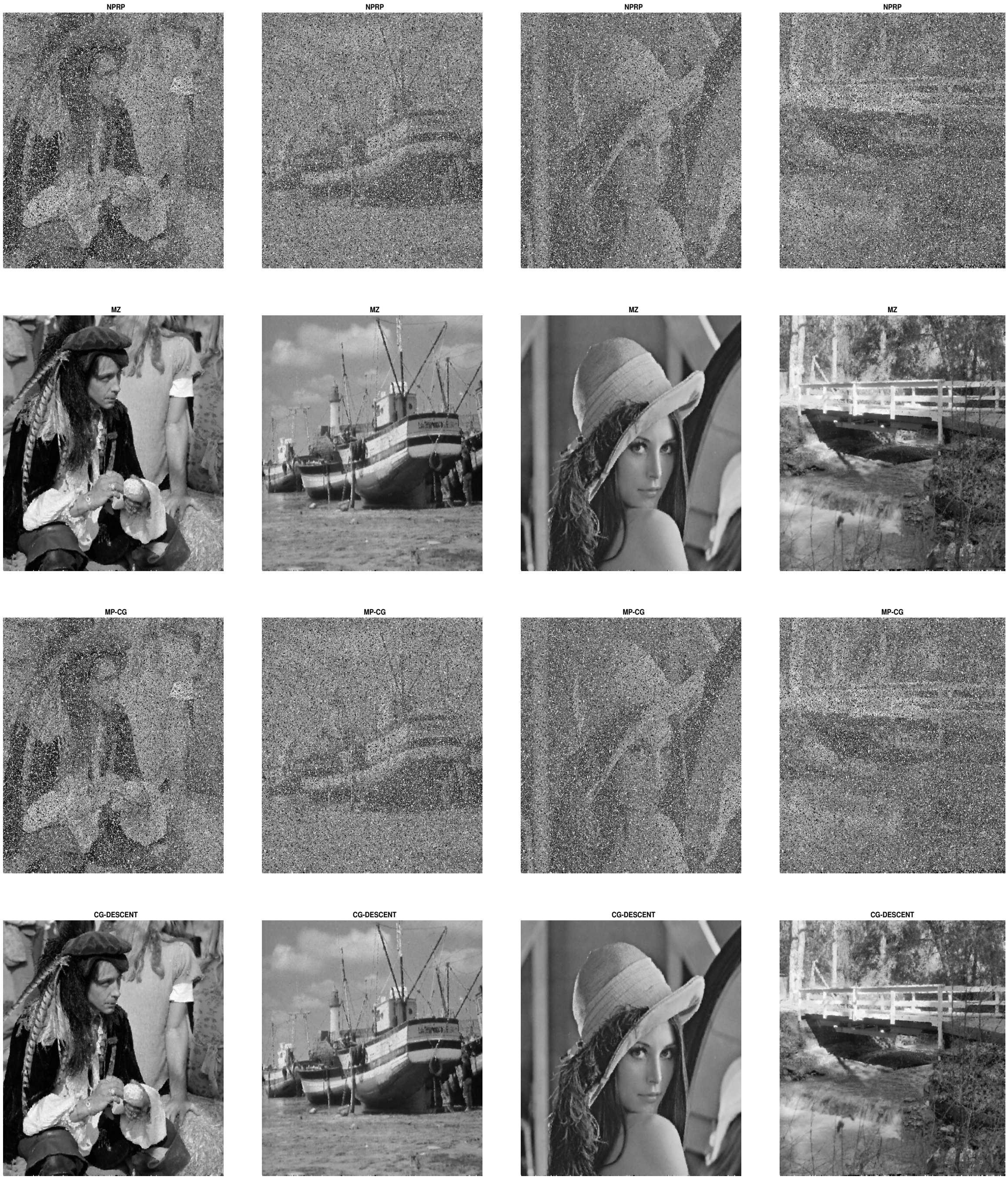

Figure 10. The restored images with 70% salt-and-pepper by NPRP (first row), MZ (second row), MP-CG (third row), and CG-DECENT (last row).

Use of AI tools declaration

We declare that we have not used Artificial Intelligence (AI) tools in the creation of this article.

Acknowledgments

The Researchers would like to thank the Deanship of Graduate Studies and Scientific Research at Qassim University for financial support (QU-APC-2025).

Conflict of interest

The authors declare there are no conflicts of interest.

References

1. R. Ziadi, A. Bencherif-Madani, A perturbed quasi-Newton algorithm for bound-constrained global optimization, *J. Comput. Math.*, **43** (2025), 143–173. https://doi.org/10.4208/jcm.2307-m2023-0016
2. R. Ziadi, A. Bencherif-Madani, A mixed algorithm for smooth global optimization, *J. Math. Model.*, **11** (2023), 207–228. https://doi.org/10.22124/JMM.2022.23133.2061
3. O. O. O. Yousif, R. Ziadi, M. A. Saleh, A. Z. Almaymuni, Another updated parameter for the Hestenes-Stiefel conjugate gradient method, *Int. J. Anal. Appl.*, **23** (2025), 10. https://doi.org/10.28924/2291-8639-23-2025-10
4. C. Souli, R. Ziadi, A. Bencherif-Madani, H. M. Khudhur, A hybrid CG algorithm for nonlinear unconstrained optimization with application in image restoration, *J. Math. Model.*, **12** (2024), 301–317. https://doi.org/10.22124/JMM.2024.26151.2317
5. Y. Chen, H. Huang, K. Huang, M. Roohi, C. Tang, A selective chaos-driven encryption technique for protecting medical images, *Phys. Scr.*, **100** (2025), 0152a3. https://doi.org/10.1088/1402-4896/ad9fad
6. K. Xiong, S. Wang, The online random Fourier features conjugate gradient algorithm, *IEEE Signal Process. Lett.*, **26** (2019), 740–744. https://doi.org/10.1109/LSP.2019.2907480
7. M. A. Saleh, Enhancing deep learning optimizers for detecting malware using line search method under strong Wolfe conditions, in *2023 3rd International Conference on Computing and Information Technology (ICCIT)*, (2023), 222–226. https://doi.org/10.1109/ICCIT58132.2023.10273908
8. M. Zhang, X. Wang, X. Chen, A. Zhang, The kernel conjugate gradient algorithms, *IEEE Trans. Signal Process.*, **66** (2018), 4377–4387. https://doi.org/10.1109/TSP.2018.2853109
9. K. Xiong, H. H. Lu, S. Wang, Kernel correntropy conjugate gradient algorithms based on half-quadratic optimization, *IEEE Trans. Cyber.*, **55** (2020), 5497–5510. https://doi.org/10.1109/TCYB.2019.2959834
10. R. Ziadi, R. Ellaia, A. Bencherif-Madani, Global optimization through a stochastic perturbation of the PolakC Ribière conjugate gradient method, *J. Comput. Appl. Math.*, **317** (2017), 672–684. https://doi.org/10.1016/j.cam.2016.12.021
11. A. Mehamdia, Y. Chaib, T. Bechouat, Two modified conjugate gradient methods for unconstrained optimization and applications, *RAIRO Oper. Res.*, **57** (2023), 333–353. https://doi.org/10.1051/ro/2023010

12. M. R. Hestenes, E. Stiefel, Methods of conjugate gradients for solving linear systems, *J. Res. Natl. Bur. Stand.*, **49** (1952), 409–436.

13. R. Fletcher, *Practical Methods of Optimization*, Wiley, New York, 1997.

14. B. T. Polyak, The conjugate gradient method in extreme problems, *USSR Comput. Math. Math. Phys.*, **9** (1969), 94–112. https://doi.org/10.1016/0041-5553(69)90035-4

15. E. Polak, G. Ribiere, Note sur la convergence de méthodes de directions conjuguées, *Rev. Française Inf. Rech. Opr.*, **16** (1969), 35–43.

16. Y. Liu, C. Storey, Efficient generalized conjugate gradient algorithms. Part 1: Theory, *J. Optim. Theory Appl.*, **69** (1992), 129–137. https://doi.org/10.1007/BF00940464

17. Y. H. Dai, Y. Yuan, An efficient hybrid conjugate gradient method for unconstrained optimization, *Ann. Oper. Res.*, **103** (2001), 33–47. https://doi.org/10.1023/A:1012930416777

18. D. Ahmed, C. Storey, Efficient hybrid conjugate gradient techniques, *J. Optim. Theory Appl.*, **64** (1990), 379–397. https://doi.org/10.1007/BF00939455

19. J. K. Liu, S. J. Li, New hybrid conjugate gradient method for unconstrained optimization, *Appl. Math. Comput.*, **245** (2014), 36–43. https://doi.org/10.1016/j.amc.2014.07.096

20. N. Andrei, Another nonlinear conjugate gradient algorithm for unconstrained optimization, *Optim. Meth. Soft.*, **24** (2008), 89–104. https://doi.org/10.1080/10556780802393326

21. X. Y. Zheng, X. L. Dong, J. R. Shi, W. Yang, Further comment on another hybrid conjugate gradient algorithm for unconstrained optimization by Andrei, *Numer. Algorithms*, **84** (2019), 603–608. https://doi.org/10.1007/s11075-019-00771-1

22. S. S. Djordjevic New hybrid conjugate gradient method as a convex combination of LS and CD methods, *Filomat*, **31** (2017), 1813–1825. https://doi.org/10.1007/s10473-019-0117-6

23. C. Souli, R. Ziadi, I. E. Lakhdari, A. Leulmi, An efficient hybrid conjugate gradient method for unconstrained optimization and image restoration problems, *Iran. J. Numer. Anal. Optim.*, **15** (2024), 99–123. https://doi.org/10.1109/LSP.2019.290748010.22067/ijnao.2024.88087.1449

24. M. Rivaie, M. Mamat, L. W. June, I. Mohd, A new class of nonlinear conjugate gradient coefficients with global convergence properties, *Appl. Math. Comput.*, **218** (2012), 11323–11332. https://doi.org/10.1016/j.amc.2012.05.030

25. Z. X. Wei, S. W. Yao, L. Y. Liu, The convergence properties of some new conjugate gradient methods, *Appl. Math. Comput.*, **183** (2006), 1341–1350. https://doi.org/10.1016/j.amc.2006.05.150

26. L. Zhang, An improved Wei-Yao-Liu nonlinear conjugate gradient method for optimization computation, *J. Appl. Math. Comput.*, **215** (2009), 2269–2274. https://doi.org/10.1016/j.amc.2009.08.016

27. I. M. Sulaiman, N. A. Bakar, M. Mamat, B. A. Hassan, M. Malik, M. A. Ahmed, A new hybrid conjugate gradient algorithm for optimization models and its application to regression analysis, *J. Electr. Eng. Comput. Sci.*, **23** (2021), 1100–1109. https://doi.org/10.11591/ijeecs.v23.i2.pp1100-1109

28. S. Yao, Z. Wei, H. Huang, A note about WYLs conjugate gradient method and its applications, *Appl. Math. Comput.*, **191** (2007), 381–388. https://doi.org/10.1016/j.amc.2007.02.094

29. I. Bongartz, A. R. Conn, N. Gould, P. L. Toint, CUTEr: A constrained and unconstrained testing environment, *ACM Trans. Math. Softw.* **29** (2003), 373–394. https://doi.org/10.1145/962437.96243

30. N. Andrei, An unconstrained optimization test functions, *Adv. Mode. Optim.*, **10** (2008), 147–161.

31. M. Hamoda, M. Mamat, M. Rivaie, Z. Salleh, A conjugate gradient method with strong Wolfe-Powell line search for unconstrained optimization, *Appl. Math. Sci.*, **10** (2016), 13–16. http://dx.doi.org/10.12988/ams.2016.56449

32. I. E. Livieris, P. Pintelas, Globally convergent modified Perrys conjugate gradient method, *Appl. Math. Comput.*, **218** (2012), 9197–9207. https://doi.org/10.1016/j.amc.2012.02.076

33. W. W. Hager, H. Zhang, A new conjugate gradient method with guaranteed descent and an efficient line search, *SIAM J. Optim.*, **16** (2005), 170–192. https://doi.org/10.1137/030601880

34. E. D. Dolan, J. J. Mor, Benchmarking optimization software with performance profiles, *Math. Program.*, **91** (2002), 201–213. https://doi.org/10.1007/s101070100263